Original Article

Assessment of the Effect of Children's Bone Density Development in Pediatric MR Only Treatment Planning

Banafsheh Zeinali Rafsanjani[1], Reza Faghihi[1, 2, *], Mahdi Saeedi Moghadam[3, 4]

1- Nuclear Engineering Department, School of Mechanical Engineering, Shiraz University, Shiraz, Iran.

2- Radiation Research Center, School of Mechanical Engineering, Shiraz University, Shiraz, Iran.

3- Ionizing and Non-Ionizing Radiation Protection Research Center, School of Paramedical Sciences, Shiraz University of Medical Sciences, Shiraz, Iran.

4- Science and Research Branch of Islamic Azad University, Tehran, Iran.

Received: 11 March 2015

Accepted: 5 August 2015

ABSTRACT

Purpose- MR only treatment planning for pediatric radiation therapy is helpful to reduce the patient dose and more precise target definition. Bone segmentation and assigning a suitable bulk electron density to bone tissue is important in this technique. Bone in children under 14 years old is still developing so the mineral density is changing during these ages. The objective of this study is to assess the effect of assigning the same bulk electron density to bone tissues of the children with different ages on dose distribution.

Methods- Seven sets of skull CT images of children under 19 years old were selected. Skull bones were segmented and the CT numbers extracted, then the CT numbers converted to density. In order to compare the differences of dose distribution due to differences in bone density, the percentage depth dose was calculated by Monte Carlo simulation in inhomogeneous phantoms.

Results- The results of PDDs in photon and electron sources did not show a significant difference (<2%) between different densities beneath the bone tissue.

Conclusion- When MR only treatment planning is to be used for a child, the bulk density method is accurate enough for treatment of brain or underneath area of bone. However, if the target of radiation therapy is bone, this method may cause a little error in dose calculation especially in superficial and electron therapy, so that voxel based methods are more reliable for these treatments.

Keywords:

Bone development,

Pediatric radiotherapy,

MR only treatment planning.

1. Introduction

Computed tomography (CT) has a significant role in 3D conformal radiotherapy but it is going to be replaced by Magnetic resonance imaging (MRI). MRI has important advantages in treatment planning in comparison to CT scan such as greater soft tissue contrast, usage of magnetic fields instead of ionizing radiation fields and more importantly the ability to provide functional information of tissue [1-3].

All of the mentioned advantages can have a key role in different steps of radiation therapy. Better soft tissue contrast can help in better target and organ at risks definition [4]. Furthermore, MRI can be used before during and after treatment for patient follow up without concerning about secondary malignancies arising from ionizing radiation [5]. Functional information from functional MRI (fMRI), diffusion weighted (DW) techniques or magnetic resonance spectroscopy (MRS) provide this ability to assess or predict the tumor response to treatment, defining the tumor stage and defining the functional target and organ at risks [4, 6-11]. MRI is going to be used as a tool for image

***Corresponding Author:**

Reza Faghihi, PhD

Medical Radiation Department, School of Mechanical Engineering, Shiraz University, Shiraz, Iran.

Tel: (+98) 7132334033 / Fax: (+98) 7136473035

E-mail: faghihir@shirazu.ac.ir

guided radiotherapy (IGRT) so that MRI-Cobalt and MRI-Linac is being developed and even they are being used in some limit radiation therapy centers [12]. Fast and dynamic MRI methods actuate radiation therapy toward IGRT using MRI [13-17].

Besides all of these advantages, MRI has some problems such as a little image distortion and the lack of electron density information which is more important. Electron density information can be provided from CT images. There are different methods to provide electron density map, one of which is the rigid registration of MRI images on CT images. Unfortunately, this method will be so difficult when patient position is a little different between MRI and CT imaging [1, 18, 19].

In order to reduce the uncertainties of rigid registration and even omit the CT imaging, MR only treatment planning was a solution. It also reduces the cost of treatment and patient dose besides of reducing the depreciation of equipment and personnel time. There are two methods for MR only planning: deformable image registration or atlas based mapping and segmentation methods [20]. Deformable image registration has a disadvantage, for example skeletal abnormalities make this method difficult. Therefore, the segmentation of different tissues and assigning a bulk density to each segment is more popular. A comparison between bulk and voxel based treatment planning has shown that assigning a bulk density to tissues can be accurate enough in some types of cancers [18]. Bone segmentation is the most important part of this technique because bone can have a significant role in dose calculation and making digitally reconstructed radiograph (DRR) [21].

MR only treatment planning for pediatric radiation therapy can be helpful as well to reduce the patient dose and more precise target definition [2]. 18% of childhood cancers are CNS cancers and 12% is bone and soft tissue sarcomas [22]. In both cases, the segmentation of bone tissues and assigning a suitable electron density to the bone segments is important. Bone in children under 14 years old is still developing, so the bone mineral density is changing during these ages [23-25].

As it is mentioned above in some MR only treatment planning systems, a bulk density is assigning to bone even for children with different ages. Now the question is whether assigning the same bulk electron density to bone tissues of children with different ages can have a significant role in dose distribution and dose calculations. In this study, we have endeavored to answer this question.

Some sets of skull CT images of children under 19 years old were selected. Skull bones were segmented and the CT numbers were extracted, then the CT numbers converted to density. In order to compare the differences of dose distribution due to differences in bone density, the percentage depth dose (PDD) was calculated by Monte Carlo simulation in inhomogeneous phantoms.

2. Materials and Methods

Seven sets of skull CT images from patients in the age range of three month to nineteen years old were selected randomly. All images were produced by the same machine (16 slice GE bright speed) and with the same slice thickness of 5 mm. Skull bone were segmented and the CT numbers of them were extracted and the average value of CT number was calculated.

In order to have a better vision of the distribution of skull bone CT numbers, cumulative bone volume histograms were created for all patients (Figure 1). Cumulative bone volume histogram demonstrates that how much of bone volume has a certain CT number or more than that.

The average value of CT numbers was converted to tissue density by CTCREAT ramp which is used in PEGS4 cross section data file. This ramp considers four materials including air, lung tissue and bone [26].

Because the relative densities of skull bones were close to each other, the bone density of four patients (3 month, 1, 8 and 19 years old) which were more different were selected for Monte Carlo simulation to calculate percentage depth dose. MCNPX version 2.5 was used for modeling. A slab of 5×5×0.5 cm^3 skull bone on a slab of 5×5×10 cm^3 brain was modeled as an inhomogeneous phantom. Three beam energies were selected for therapy source to cover all kind of radiation external therapies, x- ray of superficial energy (120 kVp), x-ray of mega voltage energy of Linac (6 MV) and 12 MeV electrons. Mesh tally type 3 were used to calculate the dose distribution in the phantom.

3. Results

The average CT number of total skull was calculated for each patient. Some variations in the average value of CT numbers was seen which can be a normal variation. For example a 6 year-old patient showed denser bones which may because of his sex and diet.

Bone volume histograms of each patient are shown in Figure 1.

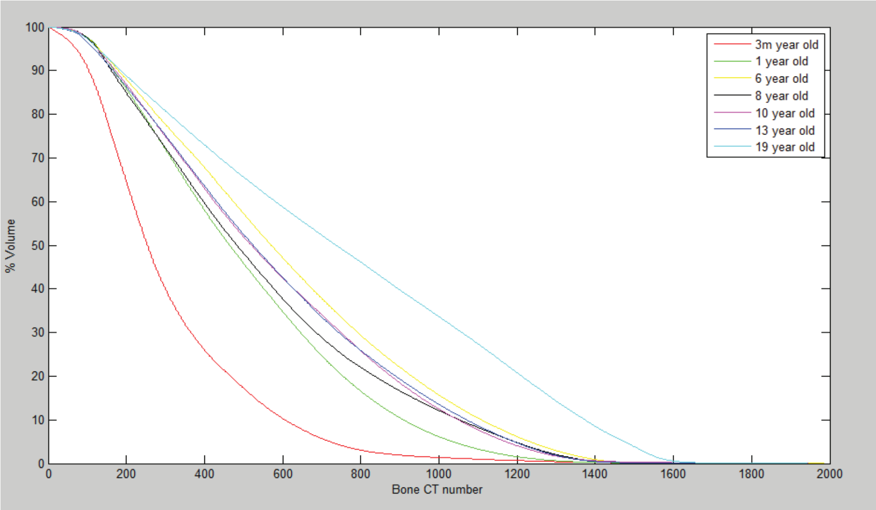

Figure 1. Cumulative bone volume histogram of all patients. Cumulative bone volume histogram demonstrates how much of bone volume has a certain CT number or more than that.

The bone densities assigned to average value of CT numbers is demonstrated in Table 1.

The results of PDD in all three sources are presented in Figure 2 to 4. The PDD curves normalized to the depth of 2 cm.

Table 1. Average CT number and relative density of skull bone for each patient.

Age	Average CT number	Relative density (g/cm^3)
3 m	313.52	1.2
1 y	508.48	1.3
6 y	611.70	1.45
8 y	546.61	1.35
10 y	572.91	1.4
13 y	575.74	1.41
19 y	762.52	1.42

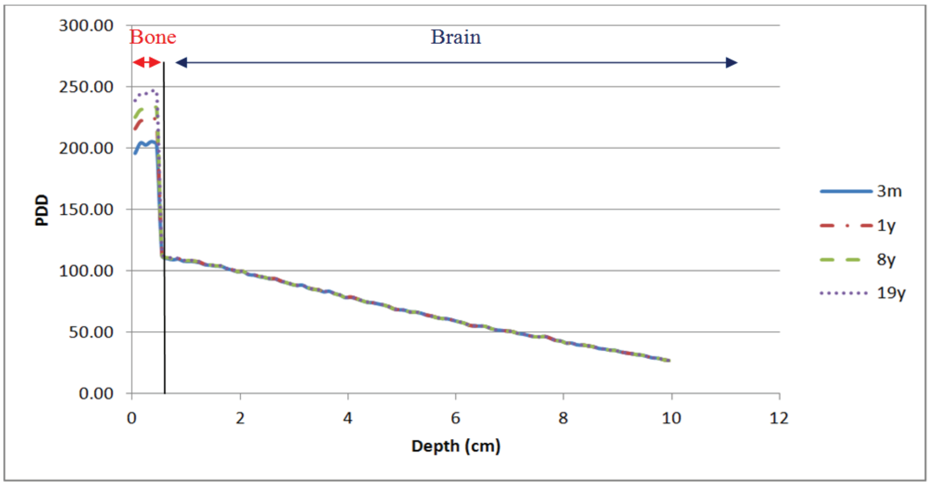

Figure 2. The result of PDD in 120 kVp x-ray in 3 month, 1, 8 and 19 year-old patients.

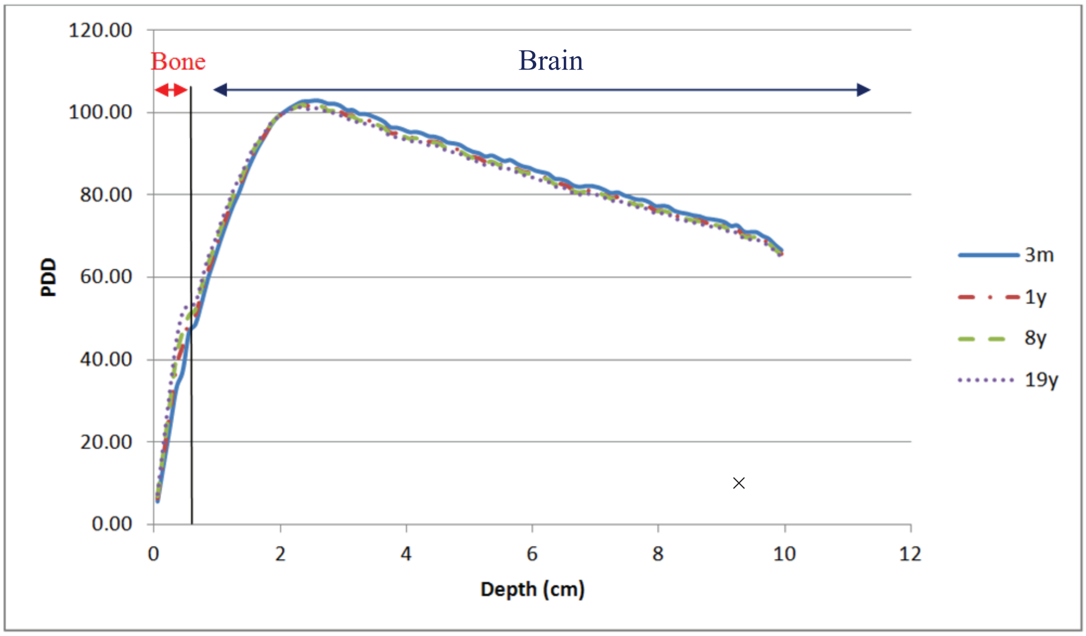

Figure 3. The result of PDD in 6 MeV x-ray in 3 month, 1, 8 and 19 year-old patients.

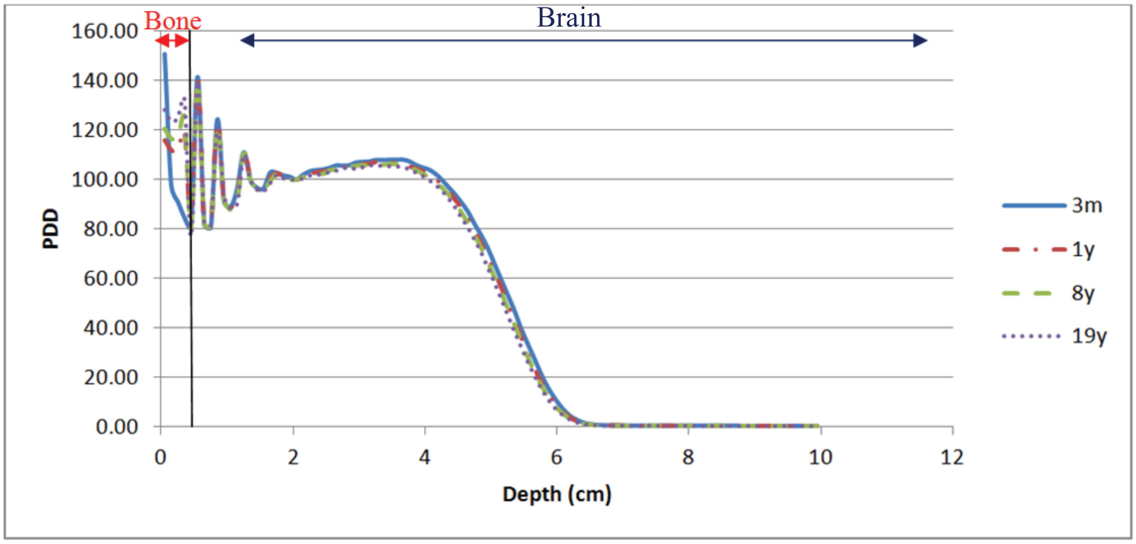

Figure 4. The result of PDD in 12 MeV electrons in 3 month, 1, 8 and 19 year-old patients.

4. Discussion

Figure 1 shows that the CT number of each age is different from the other one. It is particularly clear in Figure 1 that the distribution of bone CT numbers is different and is increasingly growing toward compact bone CT numbers by the increase of age. It is apparently because of the development of compact bones in older ages. Small CT numbers in Figure 1 relates to spongy bone and undeveloped part of bones or the area of mastoid air cavities.

Despite the obvious difference in bone CT numbers between different ages, the related density corresponding to average value of CT numbers were relatively close to each other. The result of PDDs in two different energies of photons and 12 MeV electrons revealed that the difference of CT numbers did not have a significant effect on dose distribution beneath the bone layer. The differences due to different densities just demonstrate its effect on the dose of bone layer which may be important in the treatment of bone cancers but not in brain cancers.

In 120 kVp, a significant increase in the dose of bone can be seen which is because of the photoelectric effect. In 6 MeV photons, the Compton Effect is more important so that the significant increase of bone dose cannot be seen. In 12 MeV electrons, a strong ups and falls occurred in the interface of bone and brain even up to 1 cm depth in to the brain. However, no significant effect had been seen in deeper parts. In all sources in the areas with the depth of more than 2 cm the differences of dose due to different bone densities were not more than 2 %.

The results of PDDs in all kinds of sources did not show a significant difference (<2%) between different densities beneath the bone tissue. In electron sources, different densities were more important but not in the depth of more than 1cm under the bone layer. The differences were just obvious in bone layer especially in superficial energies so that the differences between densities are important in the treatment of bone tissues. In electron therapy when the target is close to bone, the bone density also is important in the calculation of dose.

When MR only treatment planning is to be used for a child, the bulk density method is accurate enough for the treatment of brain or underneath area of bone. However, if the target of radiation therapy is bone, this method may cause a little error in dose calculation particularly in superficial and electron therapy, so that voxel based methods are more reliable for these treatments. Mega voltage photon treatment is not that much sensitive to the difference of densities but again in the treatment of bone tissues necessary care should be taken to assign a more suitable density to the bones of children.

References

1- T. Stanescu, J. Hans-Sonke, P. Stavrev, and B. G. Fallone, "3T MR-based treatment planning for radiotherapy of brain lesions," *Radiol Oncol*, vol. 40, pp. 125-32, 2006.

2- M. Koshy, M. Pentaleri, S. Paryani, C. Anderson, J. Cesaretti, A. Deshmukh, et al., "The Role of MRI in Radiation Therapy Planning," F. R. O. G. MRI Center of North Florida, Ed. Jacksonville, Florida.

3- T. Boettger, T. Nyholm, M. Karlsson, C. Nunna, and J. C. Celi, "Radiation therapy planning and simulation with magnetic resonance images " *Medical Imaging*, 2008.

4- P. Metcalfe, G. P. Liney, L. Holloway, A. Walker, M. Barton, G. P. Delaney, et al., "The potential for an enhanced role for MRI in radiation-therapy treatment planning," *Technol Cancer Res Treat*, vol. 12, pp. 429-46, Oct 2013.

5- C. M. Rank, N. Hunemohr, A. M. Nagel, M. C. Rothke, O. Jakel, and S. Greilich, "MRI-based simulation of treatment plans for ion radiotherapy in the brain region," *Radiother Oncol*, vol. 109, pp. 414-8, Dec 2013.

6- L. Nilsen, A. Fangberget, O. Geier, D. R. Olsen, and T. Seierstad, "Diffusion-weighted magnetic resonance imaging for pretreatment prediction and monitoring of treatment response of patients with locally advanced breast cancer undergoing neoadjuvant chemotherapy," *Acta Oncol*, vol. 49, pp. 354-60, Apr 2010.

7- M. V. Knopp, H. von Tengg-Kobligk, and P. L. Choyke, "Functional magnetic resonance imaging in oncology for diagnosis and therapy monitoring," *Mol Cancer Ther*, vol. 2, pp. 419-26, Apr 2003.

8- M. D. Guimaraes, A. Schuch, B. Hochhegger, J. L. Gross, R. Chojniak, and E. Marchiori, "Functional magnetic resonance imaging in oncology: state of the art*," *Radiol Bras*, vol. 47, pp. 101-11, 2014.

9- Y. Mardor, Y. Roth, A. Ochershvilli, R. Spiegelmann, T. Tichler, D. Daniels, et al., "Pretreatment prediction of brain tumors' response to radiation therapy using high b-value diffusion-weighted MRI," *Neoplasia*, vol. 6, pp. 136-42, Mar-Apr 2004.

10- E. P. Jansen, L. G. Dewit, M. van Herk, and H. Bartelink, "Target volumes in radiotherapy for high-grade malignant glioma of the brain," *Radiother Oncol*, vol. 56, pp. 151-6, Aug 2000.

11- 11- M. L. Nguyen, B. Willows, R. Khan, A. Chi, L. Kim, S. G. Nour, et al., "The potential role of magnetic resonance spectroscopy in image-guided radiotherapy," *Front Oncol*, vol. 4, p. 91, 2014.

12- G. Liney, R. Rai, L. Holloway, and S. Vinod, "A Dedicated MRI Scanner for Radiotherapy Planning: Early Experiences " *Clinical Radiation Therapy*, 2014.

13- D. Lee, S. Pollock, B. Whelan, P. Keall, and T. Kim, "Dynamic keyhole: a novel method to improve MR images in the presence of respiratory motion for real-time MRI," *Med Phys*, vol. 41, p. 072304, Jul 2014.

14- C. Plathow, H. Hof, S. Kuhn, M. Puderbach, S. Ley, J. Biederer, et al., "Therapy monitoring using dynamic MRI: analysis of lung motion and intrathoracic tumor mobility before and after radiotherapy," *Eur Radiol*, vol. 16, pp. 1942-50, Sep 2006.

15- C. Plathow, S. Ley, C. Fink, M. Puderbach, W. Hosch, A. Schmahl, et al., "Analysis of intrathoracic tumor mobility during whole breathing cycle by dynamic MRI," *Int J Radiat Oncol Biol Phys*, vol.

59, pp. 952-9, Jul 15 2004.

16- M. von Siebenthal, G. Szekely, U. Gamper, P. Boesiger, A. Lomax, and P. Cattin, "4D MR imaging of respiratory organ motion and its variability," *Phys Med Biol*, vol. 52, pp. 1547-64, Mar 21 2007.

17- J. Cai, Z. Chang, Z. Wang, W. Paul Segars, and F. F. Yin, "Four-dimensional magnetic resonance imaging (4D-MRI) using image-based respiratory surrogate: a feasibility study," *Med Phys*, vol. 38, pp. 6384-94, Dec 2011.

18- A. Karotki, K. Mah, G. Meijer, and M. Meltsner, "Comparison of bulk electron density and voxel-based electron density treatment planning," *J Appl Clin Med Phys*, vol. 12, p. 3522, 2011.

19- J. A. Dowling, J. Lambert, J. Parker, O. Salvado, J. Fripp, A. Capp, et al., "An atlas-based electron density mapping method for magnetic resonance imaging (MRI)-alone treatment planning and adaptive MRI-based prostate radiation therapy," *Int J Radiat Oncol Biol Phys*, vol. 83, pp. e5-11, May 1 2012.

20- R. Prabhakar, P. K. Julka, T. Ganesh, A. Munshi, R. C. Joshi, and G. K. Rath, "Feasibility of using MRI alone for 3D radiation treatment planning in brain tumors," *Jpn J Clin Oncol*, vol. 37, pp. 405-11, Jun 2007.

21- H. M. Kjer, "MRI in radiation therapy planning: the use of ultrashort echo time imaging," Technical University of Denmark, Informatics and Mathematical Modelling, Technical University, Denmark, 2012.

22- D. G. Kirsch and N. J. Tarbell, "Conformal radiation therapy for childhood CNS tumors," *Oncologist*, vol. 9, pp. 442-50, 2004.

23- J. Tamayo, R. Diaz, E. Lazcano-Ponce, M. Munoz, G. Huitron, E. Halley, et al., "Reference values for areal bone mineral density among a healthy Mexican population," *Salud Publica Mex*, vol. 51 Suppl 1, pp. S56-83, 2009.

24- L. R. Yeh, C. K. Chen, and P. H. Lai,"Normal bone mineral density in anteroposterior, lateral spine and hip of Chinese men in Taiwan: effect of age change, body weight and height," *J Chin Med Assoc*, vol. 67, pp. 287-95, Jun 2004.

25- B. S. Zemel, H. J. Kalkwarf, V. Gilsanz, J. M. Lappe, S. Oberfield, J. A. Shepherd, et al., "Revised Reference Curves for Bone Mineral Content and Areal Bone Mineral Density According to Age and Sex for Black and Non-Black Children: Results of the Bone Mineral Density in Childhood Study," *J Clin Endocrinol Metab*, vol. 96, pp. 3160-3169, 2011.

26- B. Walters, I. Kawrakow, and DWO. Rogers, "DOSXYZnrc users manual," 2005.